Renormalization Group Approach to Spectral Properties of the Two-Channel Anderson Impurity Model

Frithjof B. Anders
Department of Physics, Universität Bremen, P.O. Box 330 440, D-28334 Bremen, Germany
(Dated: 7-07-2004)

The impurity Green function and dynamical susceptibilties for the two-channel Anderson impurity model are calculated. An exact expression for the self-energy of the impurity Green function is derived. The imaginary part of the self-energy scales as $\sqrt{|\omega/T_K|}$ for $T \to 0$ serving as a hallmark for non-Fermi behavior. The many-body resonance is pinned to a universal value $1/(2\pi\Delta)$ at $\omega = 0$. Its shape becomes increasingly more symmetric for the Kondo-regimes of the model. The dynamical susceptibilities are governed by two energy scales T_K and T_h and approach a constant value for $\omega \to 0$, whereas relation $\chi''(\omega) \propto \omega$ holds for the single channel model.

PACS numbers: 71.10.Hf, 71.27.+a, 71.20.Eh

Introduction: In the last decade, the paradigm of a Fermi-liquid ground state in Heavy Fermion (HF) materials [1], which originally gave these mainly Ce and Uranium base compounds their name, has become strongly questioned. In addition to magnetic and superconducting phase transitions, many of these alloys show deviations from the Fermi-liquid behavior in the normal phase. Typically, logarithmic behavior and power laws with anomalous exponents have been reported in the low-temperature thermodynamic and transport properties [2]. These unusual properties are attributed to charge and spin fluctuations on the partially filled f-shells. Certain ballistic metallic point contacts, two-level systems[3] and coupled quantum-dot[4] have been argued to display similarly unusual properties.

While the $4f$-shell of Ce ions is usually occupied by one electron, the configuration of the $5f$-shell of U ions fluctuates between degenerate $5f^2$ and $5f^3$ crystal field states. Hund's rules coupling and crystal field splitting in a cubic symmetry yield a Kramer's degenerate Γ_6 ground state $|\sigma\rangle$ for the $5f^3$ and a quadrupolar $5f^2$-Γ_3 doublet $|\alpha\rangle$. On symmetry grounds, these states only hybridized with Γ_8 conduction electron labelled by a spin σ and channel index α[5]. The Hamiltonian of this two-channel Anderson impurity model (TC-SIAM) is given by

$$\mathcal{H} = \sum_{k\alpha\sigma} \varepsilon_{k\alpha\sigma} c^\dagger_{k\alpha\sigma} c_{k\alpha\sigma} + \sum_\sigma (E_\sigma - E_\alpha) X_{\sigma,\sigma} + h_s S_z + h_c \tau_z + \sum_{k\alpha\sigma} V_\alpha \left(X_{\sigma,-\alpha} c_{k\alpha\sigma} + c^\dagger_{k\alpha\sigma} X_{-\alpha,\sigma} \right) \quad (1)$$

where the operator $c^\dagger_{k\alpha\sigma}$ creates an electron with energy $\varepsilon_{k\alpha\sigma}$, momentum k, quadrupolar channel $\alpha = \pm$ and spin σ. $X_{m,m'} = |m\rangle\langle m'|$ is the usual Hubbard operator which destroys the ionic state $|m'\rangle$ and creates the ionic state $|m\rangle$. The energy E_σ is assigned to the magnetic doublet, the energy E_α to the quadrupolar doublet containing one electron less than $|\sigma\rangle$. The last term describes the hybridization between the f-shell and the conduction electron host. The external magnetic and channel fields, h_s and h_c, couple to the local spin or channel flavor operator, $S_z = \sum_\sigma \sigma X_{\sigma\sigma}/2$, and $\tau_z = \sum_\alpha \alpha X_{\alpha\alpha}/2$ and are used to calculate the local spin- or channel susceptibility $\chi_s = \frac{\langle S_z\rangle}{h_s}$ or $\chi_c = \frac{\langle \tau_z\rangle}{h_c}$, respectively, for $h_s, h_c \to 0$. This model was proposed in the context of UBe_{13} by Cox[3, 5] for a novel and unusual Kondo effect: the non-magnetic $5f^2$-Γ_3 ground state undergoes a quadrupolar charge rather than a magnetic Kondo-screening. Using a Monte-Carlo approach[6], it was shown that (i) the magnetic and quadrupolar moments are screened for $T \to 0$, (ii) this screening is described by two different energy scales $T_h \geq T_l \to T_K$, (iii) both channel and spin susceptibility behave as $\chi_{s/c} \propto \ln(T)$ in the universality regime $T \ll T_l$. Recently, this was confirmed by an exact Bethe *ansatz* solution[7] of the model (1). It was also possible to calculate the threshold exponents of the resolvent $I_M(z) = \langle M, 0|1/(z - \hat{H})|M, 0\rangle \approx I_0(z - E_g)^{-\alpha_M}$ of the time evolution of the local levels $M = \sigma, \alpha$ relative to the Fermi-see of the free electron gas[8]; E_g is the threshold energy. In contrary to the non-Crossing Approximation (NCA)[3, 5, 9, 10] predicting $\alpha_M = 1/2$, the true exponents are dependent on the occupation of $n_c = \sum_\sigma \langle X_{\sigma\sigma}\rangle$. Since the Green function $G_{\alpha\sigma}(z) = \ll X_{\alpha,\sigma}|X_{\sigma,\alpha} \gg$ is obtained by a convolution of $I_\sigma(z)$ and $I_\alpha(z)$ in NCA [5], its spectral function would be given by $\rho_{\alpha\sigma}(\omega) = \rho_0^\pm |\omega|^{1-\alpha_\sigma-\alpha_\alpha} B(1-\alpha_\sigma, 1-\alpha_\alpha) \propto \rho_0^\pm |\omega|^{-\frac{1}{2}n_c(n_c-1)}$ for $|\omega| \to 0$ using the exact threshold exponents[11]; B is the beta function. Hence, the spectral function should diverge for $n_c \neq 0, 1$, indicating that vertex corrections are as important as the exact exponents α_M for obtaining the correct spectral function from $I_M(z)$[12].

In this Letter, the first accurate solution for the dynamical properties of the model using Wilson's numerical renormalization-group method (NRG)[13] is presented. It is shown that (i) the scaling behavior of $\rho_{\alpha\sigma}(\omega)$ is given by $(1 - a_\pm\sqrt{|\omega|/T_K})$ with a very weak n_c dependence of the constants $a_\pm$, (ii) the many-body resonance becomes increasingly more symmetric in the Kondo regime in contrast to the NCA result, (iii) the total self-energy consists of a resonant level term and a local non-Fermi

liquid self-energy with vanishing imaginary part at $\omega = 0$, (iv) the dynamical spin and channel susceptibility $\chi''(\omega)$ approach a constant for $|\omega| < T_K$ and $T \ll T_K$, corresponding to logarithmically divergent $\chi(T)$ for $T \to 0$.

The Hamiltonian (1) is solved using the NRG[13]. The core of the NRG approach is a logarithmic energy discretization of the conduction band around the Fermi energy, $\omega_n^\pm = \pm D\lambda^{-n}$ and $\Lambda > 1$, and a unitary transformation of the base $c_{\omega_n^\pm \alpha\sigma}$ onto a base such that the Hamiltonian becomes tridiagonal. The first operator $f_{0\alpha\sigma}$ is defined as $f_{0\alpha\sigma} = \frac{1}{2}\sum_n (c_{\omega_n^+\alpha\sigma} + c_{\omega_n^-\alpha\sigma})$ [13]. Only $f_{0\alpha\sigma}$ couples directly to the impurity degrees of freedom. Eqn. (1) is recasted as a double limit of a sequence of dimensionless NRG Hamiltonians:

$$\mathcal{H} = \lim_{\Lambda\to 1^+} \lim_{N\to\infty} \left\{ D_\Lambda \Lambda^{-(N-1)/2} \mathcal{H}_N \right\}, \qquad (2)$$

with D_Λ equal to $D(1+\Lambda^{-1})/2$, and

$$\begin{aligned} \mathcal{H}_N &= \Lambda^{\frac{N-1}{2}} \left[\frac{E_{\alpha\sigma}}{D_\Lambda} \sum_\sigma X_{\sigma,\sigma} + \sum_{\sigma\alpha} \left\{ \tilde{V}_\alpha f^\dagger_{\alpha\sigma 0} X_{-\alpha\sigma} + \text{H.c.} \right\} \right. \\ &\quad \left. + \sum_{n=0}^{N-1} \sum_{\alpha\sigma} \Lambda^{-\frac{n}{2}} \xi_{n\alpha} \left\{ f^\dagger_{\alpha\sigma n+1} f_{\alpha\sigma n} + \text{H.c.} \right\} \right]. \end{aligned}$$

$\tilde{V}_\alpha$ is related to the hybridization width $D_\Lambda \tilde{V}_\alpha = V_\alpha$, $\Delta E = E_{\alpha\sigma} = E_\sigma - E_\alpha$, while the pre-factor $\Lambda^{(N-1)/2}$ guarantees that the low-lying excitations of $\mathcal{H}_N$ are of order one for all N[13]. In the absence of a symmetry breaking channel or magnetic field, the Hamiltonian has three fixed points: the free orbital fixed point H^*_{FO} with $\Delta E = 0, V = 0$, the two local moment fixed points H^*_{LM}, $|\Delta E| \to \infty, V = 0$ [14] and an intermediate coupling or two-channel fixed point H^*_{tc} governing the universality regime of the model for $T \to 0$. H^*_{FO} is instable with respect to the two relevant operators $X_{\sigma\sigma}$ and the hybridization. the local moment fixed point is instable with respect to the Kondo interaction H_K, which is either of spin type when $\Delta E < 0$, or of channel type when $\Delta E > 0$. There are two cross-over energy scales in the problem: the high temperature scale T_h, associated with the screening of the upper doublet, and the low temperature scale $T_l = T_K$, the Kondo temperature, associated with the screening of the lower doublet. The latter temperature is exponentially dependent on $\Delta/|E_{\alpha\sigma}|$, and the Bethe *ansatz* [7] predicts $T_K = \frac{4\Delta}{\pi^2}\exp[-\frac{\pi|\Delta E|}{2\Delta}]$ for the wide band limit. Introducing the hybridization function $\Gamma_{\alpha\sigma}(z) = \sum_k V_\alpha|^2/(z - \varepsilon_{k\alpha\sigma})$, the imaginary part at $\omega = -i\delta$ is denoted by $\Delta = \Delta_{\alpha\sigma} = \Im m \Gamma_{\alpha\sigma}(-i\delta)$.

Thermodynamic results: A symmetric and constant band density $\rho_0 = 1/(2D)$, a band width of $D = 10\Delta$, and a NRG discretization parameter $\Lambda = 3.5$ was chosen. All energies are measured in units of the Anderson width Δ. At each NRG iteration, $N_s = 3000$ states are kept. The impurity entropy S_{imp} is defined as the difference of the entropy of (1) with or without the quantum impurity [13]: $S_{imp} = S_{full} - S_{free}$. It is plotted for different values of $|\Delta E|$ in the upper part of Fig. 1 and agrees excellently with the Bethe ansatz results[7]. For large values of $|\Delta E/\Delta| \gg 1$, the reduction of the entropy from $\log(4) \to \log(2)$ occurs on the scale T_h, while the two-channel fixed point is approached below T_K[6, 7]. Even though the two-channel fixed point is always characterized by a residual entropy of $\frac{1}{2}\log(2)$, the NRG level spectrum of the fixed-point is non-universal and dependent on ΔE or the occupation number n_c. Since the model lacks particle-hole symmetry away from $\Delta E = 0$, the additional marginal operator, $H_m = K(\sum_{\alpha\sigma} f^\dagger_{\alpha\sigma 0} f_{\alpha\sigma 0} - 2)$ [14], leads to a line of fixed point Hamiltonians comprising of $H^*_{tc}(\Delta E = 0)$ and H_m. The constant K can be extracted from the NRG level spectra and contains the n_c-dependence [14].

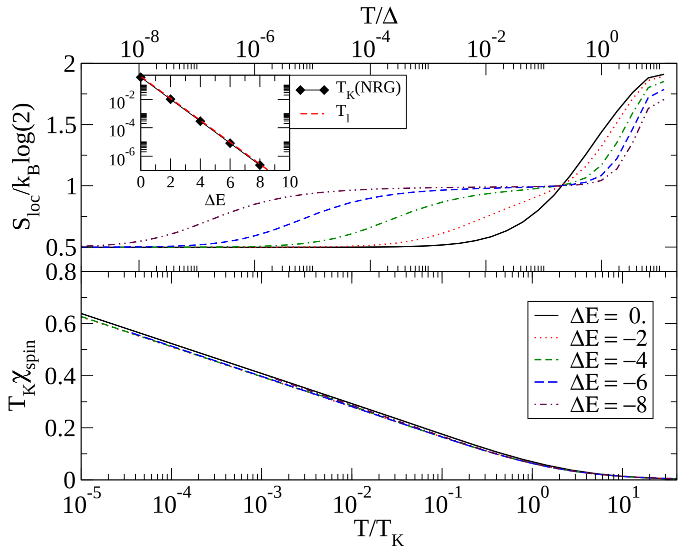

FIG. 1: Entropy vs temperature for different values of $\Delta E = E_{\alpha\sigma}$. For $|\Delta E/\Delta| \ll 1$, the Hamiltonian flows directly from the free orbital fixed point H^*_{FO} ($S_{FO} = k_B\log(4)$) to the two channel fixed-point ($S_{tc} = \log(2)/2$). For large values $|\Delta E/\Delta| \gg 1$, the Hamiltonian crosses over to the local moment fixed point ($S_{LM} = \log(2)$) first, before reaching the line of two channel fixed-points H^*_{tc}. T_K associated with the quenching of the lower doublet is shown in the inset. Parameters: $D = 10$, $N_s = 3000$, $\Lambda = 3.5$.

The logarithmically divergent susceptibilities to the low temperature form $\chi(T) = -\frac{1}{20T_K}\log(T) + b$ was fitted to extract T_K. T_K can also be defined as the temperature at which the effective moment of the lower doublet, $\mu^2_{eff}(T) = T\chi(T)$, is reduced to $\mu^2_{eff}(T_K) = 0.07$ [14]. These two temperatures coincide within the numerical error. The local spin susceptibility χ_s for $\Delta E \le 0$, or channel susceptibility χ_c for $\Delta E \ge 0$ is plotted in the lower graph of Fig. 1 for five different values of ΔE as a function of T/T_K, to illustrate the scaling. The inset shows the exponential behavior of $T_K(NRG)$ and the excellent agreement with the Bethe ansatz wide band limit $T_K = \frac{4\Delta}{\pi^2}\exp[-\frac{A_\lambda \pi|\Delta E|}{2\Delta}]$, taking into account the dis-

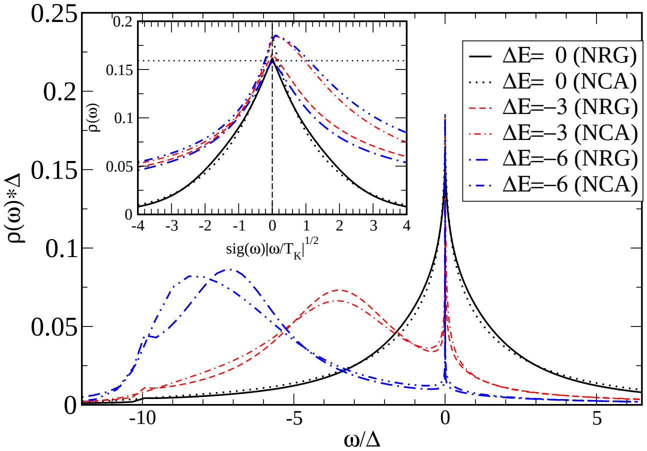

FIG. 2: NRG spectral functions for three different values of ΔE at $T=0$ in comparison with NCA spectral functions. The inset shows the behavior for $|\omega| \leq T_K$. The dotted lines marks $1/(2\pi\Delta)$. For increasing $|\Delta E|$, the peak of the NRG spectrum becomes more symmetric and approaches a universal curve. The NCA spectra are calculated at $T = 10^{-6}T_K$ for $\Delta E = 0, 3$ and $T = 10^{-3}T_K$. The value of T_K are $0.405285, 3.6 * 10^{-3}, 3.3 * 10^{-5}$ for $\Delta E = 0, -3, -6$. Parameters: $D = 10$, $N_s = 3000$, $\Lambda = 2.2$.

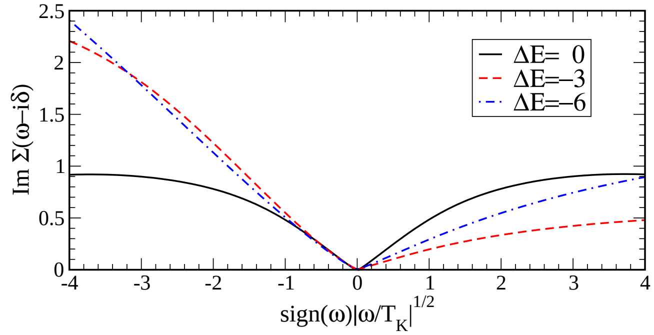

FIG. 3: Imaginary part of the self-energy $\Sigma(\omega - i\delta)$ as function of $\text{sign}(\omega)\sqrt{|w/T_K|}$ for same three different values of $\Delta E = E_{\alpha\sigma}$ at $T = 0$ and parameters as Fig. 2.

cretization correction $A_\Lambda = \frac{1}{2}\frac{1+1/\Lambda}{1-1/\Lambda}\log\Lambda$ for the Kondo coupling [14]: $J \to J_{eff} = J/A_\Lambda$.

Dynamical properties: Using the equation of motion for Fermionic Green functions, $z \ll A|B \gg = \langle\{A, B\}\rangle + \ll [A, H]|B\gg$, the commutators of the operators $X_{\alpha,\sigma}$ and $c_{k,\alpha\sigma}$ with the Hamiltonian, $[X_{\alpha,\sigma}, H]$ and $[c_{k,\alpha\sigma}, H]$ respectively, and the local completness $\sum_\sigma X_{\sigma\sigma} + \sum_\alpha X_{\alpha\alpha} = 1$, it is straight forward to derive

$$
\begin{aligned}
[z - E_{\alpha\sigma} - \Gamma_{\alpha\sigma}] \ll X_{\alpha,\sigma}|X_{\sigma,\alpha}\gg \;&=\\
P_{\alpha\sigma} + \ll \hat{O}_{\alpha\sigma}|X_{\sigma,\alpha}\gg \;&. \qquad (3)
\end{aligned}
$$

The expectation value of anti-commutator $P_{\alpha\sigma} = \langle X_{\alpha,\alpha}\rangle + \langle X_{\sigma,\sigma}\rangle$ is alway 1/2 in the absence of a symmetry breaking field. The local composite operator $\hat{O}_{\alpha\sigma}$

$$
\begin{aligned}
\hat{O}_{\alpha\sigma} \;=\; &\sum_k V_{-\alpha}\left(X_{-\sigma,\sigma}c_{k-\alpha-\sigma} - X_{-\sigma,-\sigma}c_{k-\alpha\sigma}\right)\\
&+ \sum_k \left(V_\alpha X_{\alpha,-\alpha}c_{k\alpha\sigma} - V_{-\alpha}X_{-\alpha,-\alpha}c_{k-\alpha\sigma}\right) \quad (4)
\end{aligned}
$$

also transforms as $X_{\alpha,\sigma}$. If the Green function $G_{\alpha\sigma}(z)$ is parameterized by the self-energy $\Sigma_{\alpha\sigma}(z)$, $G_{\alpha\sigma}(z) = P_{\alpha\sigma}[z - E_{\alpha\sigma} - \Gamma_{\alpha\sigma} - \Sigma_{\alpha\sigma}(z)]^{-1}$, this self-energy is given by the exact relation

$$
\Sigma_{\alpha\sigma}(z) \;=\; M_{\alpha\sigma}(z)/G_{\alpha\sigma}(z) \;, \qquad (5)
$$

defining $M_{\alpha\sigma}(z) = \ll O_{\alpha\sigma}|X_{\sigma,\alpha}\gg$. In contrary to the single channel model[15], there exists no non-interacting limit, and the spectral weight is reduced to $P_{\alpha\sigma} = 1/2$.

It is straight forward to calculate the matrix elements of operator $\hat{O}_{\alpha\sigma}$ within the NRG. The spectral functions for $M_{\alpha\sigma}$ and $G_{\alpha\sigma}$ are obtained from their Lehmann representation by broading the δ-function of the discret spectrum on a logarithmic scale, i. e. $\delta(\omega - E) \to e^{-b^2/4}e^{-(\log(\omega/E)/b)^2}/(\sqrt{\pi}b|E|)$ [15]. The broadening parameter is usually chosen as $0.5 < b < 1$, and we used $b = 0.8$. The self-energy $\Sigma(z)$ is then calculated through (5). Fig. 2 shows the spectral function $\rho_{\alpha\sigma}(\omega)$ in comparison with the results obtain by the NCA[5]. The overall agreement between the NRG and NCA curves for the same parameter is reasonably good in spite of the incorrect threshold exponents of the NCA. The NRG tends to overestimate the broadening of the high energy peaks at $\omega \approx \Delta E$, but produces highly accurate results for small frequencies $|\omega| < T_K$. The inset of Fig. 2 depicts the many-body resonance in the region for $|\omega/T_K| < 10$ on a rescaled axis $|\omega/T_K|^{1/2}$. It highlights three major aspects of spectral function: (i) $\rho(\omega) \propto 1 - a_\pm|\omega/T_K|^{1/2}$ for $|\omega| < T_K$, (ii) for increasing $|\Delta E|$, the spectral function becomes more symmetric around $\omega = 0$ and should approach a universal curve, (iii) the peak value is pinned to $1/(2\pi\Delta)$ at $\omega = 0$ independent of ΔE. Even though the vertex correction to the NCA spectra vanishes only in the limit of large spin and channel degeneracy N and M[16], the scaling behavior of the NCA spectra is apparently correct. The NCA peak, however, saturates at $\pi/(16\Delta)$ for $T \to 0$ [3] and remains asymmetric for $|\Delta E| \gg \Delta$.

Fig. 3 shows the corresponding imaginary part of the NRG self-energy $\Sigma(\omega - i\delta)$: it vanishes at $\omega = 0$, independent of ΔE, which is a neccessary condition for the pinning of the spectral function for all values of ΔE. In addition, $\Re e\Sigma(0) + \Delta + E_{\alpha\sigma} = 0$, leading to the pinning of the resonance to $\omega = 0$, depicted in Fig. 2. In the scaling regime $|\omega/T_K| < T_h$, $\Im m\Sigma(\omega - i\delta) \propto \sqrt{|\omega/T_K|}$. This region extends to multiples of $|\omega/T_K|$ for $T_h \gg T_K$. The definition of the self-energy via the parameterization of $G_{\alpha\sigma}(z)$ turns out to be very useful for the understanding of its properties. The conformal field theory result for the T-matrix of two-channel Kondo model [17]

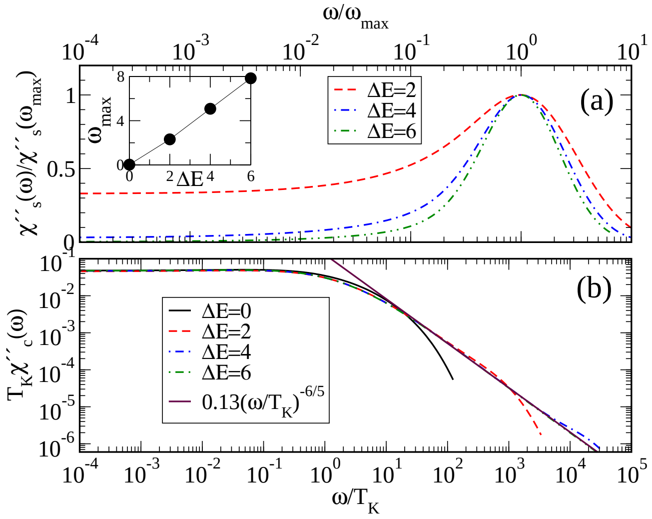

FIG. 4: Imaginary part of $\chi_s''(\omega)$ (a) scaled to position and value of the finite frequency maximum $\omega_{max} \approx T_h$ as displayed in the inset; the values of $\chi_s''(\omega_{max})$ are $0.0126, 0.0046, 0.00235$ for $\Delta E = 2, 4, 6$. The scaling curve (b) for $\chi_c''(\omega)$ vs ω/T_K at $T = 0$ for $\Delta E \geq 0$. Parameters as Fig. 2.

conveys to the TC-SIAM. The self-energy $\Sigma(z)$ exhibits similar features as the correlation self-energy $\Sigma^U(z) = \Sigma(z) - \Gamma(z)$ of the single-channel model: its imaginary part also vanishes for $\omega \to 0$ and its scaling behavior reflects the nature of the local electronic excitation. While $\Im m\Sigma(\omega - i\delta) \propto (\omega/T_K)^2$ in the single channel model, the scaling as $\Im m\Sigma(\omega - i\delta) \propto \sqrt{|\omega/T_K|}$ represents the hallmark of a local non-Fermi liquid.

The imaginary parts of the dynamical impurity spin and quadrupolar or charge susceptibility, $\chi_s(\omega) = \ll \hat{s}_z|\hat{s}_z\gg$ and $\chi_c(\omega) = \ll\hat{\tau}_z|\hat{\tau}_z\gg$ respectively, are plotted in Fig. 4 for $T = 0$ and positive $\Delta E \geq 0$. Since the Hamiltonian is symmetric with respect to a particle-hole transformation, and simmultanious $\Delta E \to -\Delta E$ and interchanging the spin and quadrupolar indices, Fig. 4 also contains the information for $\Delta E < 0$. Both χ'' show two frequency regimes. In contrast to the single channel model where the relation $\chi'' \propto \omega$ holds, $\chi''_{s/c}(\omega)$ approachs a constant at low frequencies, $|\omega| < T_K$. This corresponds to the logarithmic divergence of *both* $\chi(T)$ for $T < T_K$, and the slope of the logarithm is given by this constant. A scaling curve is found for the charge susceptibility (or spin susceptibility for $\Delta E < 0$) when plotted in dimensionless units of the low temperature scale T_K, as shown in Fig. 4 (b). The scaling holds for $\omega/T_h < 1$ above which non-universal band edge effects govern the physics. The intermediate frequency range $T_K < |\omega| < T_h$ is characterised by a power law behavior: $\chi_c''(\omega) \propto (\omega/T_K)^{-1.2}$. The peak position in $\chi_s''(\omega)$ scales with T_h and corresponds to ΔE for large ΔE [6, 7]. The values of $\chi_s''(\omega_{max})$ become increasing smaller with reduction of the occupance of the spin-doublet.

Discussion and Conclusion: The dynamical properties of the two-channel Anderson model were accuratly calculated for $T = 0$ using the NRG approach. The analytical form of the spectral function is given by $1/(2\pi\Delta)(1 - a_\pm\sqrt{\omega/T_K})$ for $|\omega| < T_K$. Its peak is pinned to a universal value, and the self-energy scales as $\sqrt{\omega/T_K}$ independent of n_c. Since the self-energy $\Sigma(z)$ does not contain the resonant level part $\Delta_{\alpha\sigma}$, and $\Im m\Sigma(\omega - i\delta) \to 0$ for $\omega \to 0$, its anomalous scaling serves as a hallmark for local non-Fermi liquid behaviour. The NCA result for the spectral function agrees remarkably well with the accurate NRG result. The two energy scales characterising the screening of the moments of upper and lower doublets also appear as charge exitation energy and as effective width of the many-body resonance at $\omega = 0$ in the spectral function. At finite temperatures - not shown here - the many-body resonance decreases for inceasing temperature and vanishes for $T \gg T_K$. The dynamical susceptibility of the lower doublet maps to a universal scaling curve for $\omega < \min\{D, T_h\}$ and $T = 0$, while a peak at $\omega_{max} \approx T_h$ is found in the dynamical susceptibility of the upper doublet.

We have benefited greatly from fruitful discussions with N. Andrei, C. Bolech and A. Schiller and would like to acknowledge the funding of the NIC, Forschungszentrum Jülich, under project no. HHB00.

[1] N. Grewe and F. Steglich, in *Handbook on the Physics and Chemistry of Rare Earths*, edited by J. K. A. Gschneidner and L. Eyring (North-Holland, Amsterdam, 1991), Vol. 14, p. 343.
[2] G. R. Stewart, Rev. Mod. Phys **73**, 797 (2001).
[3] D. L. Cox and A. Zawadowski, Advances in Physics **47**, 599 (1998), for a review on the multi-channel models.
[4] F. B. Anders et. al., cond-mat/0311502
[5] D. L. Cox, Phys. Rev. Lett. **59**, 1240 (1987).
[6] A. Schiller, F. B. Anders, and D. L. Cox, Phys. Rev. Lett. **81**, 3235 (1998).
[7] C. J. Bolech and N. Andrei, Phys. Rev. Lett. **88**, 237206 (2002).
[8] H. Johannesson, A. Andrei, and C. J. Bolech, Phys. Rev. B **68**, 075112 (2003).
[9] N. Grewe, Z. Phys. B **52**, 193 (1983).
[10] Y. Kuramoto, Z. Phys. B **53**, 37 (1983).
[11] T. A. Costi, P. Schmitteckert, J. Kroha, and P. Wölfe, Phys. Rev. Lett. **73**, 1275 (1994).
[12] F. B. Anders, J. Phys.: Condens. Matter **7**, 2801 (1995).
[13] K. G. Wilson, Rev. Mod. Phys. **47**, 773 (1975).
[14] H. R. Krishna-Murty, J. W. Wilkins, and K. G. Wilson, Phys. Rev. B **21**, 1003 (1980), ibid, **21**, 1044 (1980).
[15] R. Bulla, A. C. Hewson, and T. Pruschke, J. Phys.: Condens. Matter **10**, 8365 (1998).
[16] D. L. Cox and A. E. Ruckenstein, Phys. Rev. Lett. **71**, 1613 (1993).
[17] A. W. W. Ludwig and I. Affleck, Phys. Rev. Lett. **57**, 3160 (1991).